ISSN 1063-7834, Physics of the Solid State, 2008, Vol. 50, No. 11, pp. 2190–2198. © Pleiades Publishing, Ltd., 2008.
Original Russian Text © Yu.M. Yarmoshenko, T.V. Kuznetsova, A.V. Postnikov, A.N. Titov, S.G. Titova, V.V. Fedorenko, P. Vimercati, A. Goldoni, R. Claessen, 2008, published in Fizika Tverdogo Tela, 2008, Vol. 50, No. 11, pp. 2098–2105.

LOW-DIMENSIONAL SYSTEMS AND SURFACE PHYSICS

Spatial Dependence of the Dichroism of Photoemission of $Fe_{1/4}TiTe_2$ upon Excitation with Circularly Polarized Radiation

Yu. M. Yarmoshenko[a], T. V. Kuznetsova[a], A. V. Postnikov[b], A. N. Titov[a], S. G. Titova[c], V. V. Fedorenko[a], P. Vimercati[d], A. Goldoni[d], and R. Claessen[e]

[a] *Institute of Metal Physics, Ural Division, Russian Academy of Sciences, ul. S. Kovalevskoĭ 18, Yekaterinburg, 620219 Russia*

e-mail: yarmoshenko@ifmlrs.uran.ru

[b] *Laboratoire de Physique des Milieux Denses, Paul Verlaine University–Institute de Physique Electronique et Chimie, Metz, F-57078 France*

[c] *Institute of Metallurgy, Ural Division, Russian Academy of Sciences, ul. Amundsena 101, Yekaterinburg, 620016 Russia*

[d] *Elettra Synchrotron Light Source, Basovizza, Trieste, 34012 Italy*

[e] *Experimentalphysik II, Universität Augsburg, Augsburg, D-86135 Germany*

Received October 10, 2007; in final form, March 20, 2008

Abstract—This paper reports on the results of the experimental investigation into the angular dependence of the photoemission of the valence band (the angle-resolved photoelectron spectrum) for the $Fe_{1/4}TiTe_2$ single crystal upon excitation with circularly polarized radiation. The angle-resolved photoelectron spectrum is studied in the vicinity of the Γ point of the Brillouin zone in the two directions ΓK and ΓM with the highest symmetry. The measurements are performed in the noncoplanar geometry. The circular dichroism in the photoemission angular distribution is observed over the entire ranges of energies and angles. The magnitude of the dichroism depends on the choice of the band, the binding energy, and the polar angle and varies from 0 at the Γ point to 20%.

PACS numbers: 73.20.At, 79.60.-i

DOI: 10.1134/S1063783408110309

1. INTRODUCTION

Intercalation compounds of titanium dichalcogenides are formed through the intercalation of different objects into the interlayer space of the host lattice of TiX_2 compounds (X = S, Se, Te). If this object is represented by a 3d metal atom, it has spin-polarized valence electrons [1]. Since the interaction of exciting radiation with electrons depends on the orientation of the spin of the valence shell, the spin subbands in the case of magnetic ordering can be experimentally determined from the photoemission spectra. This can be achieved when the circularly polarized radiation with the opposite direction of polarization is used to excite photoemission. Apart from the spin polarization, there are other factors responsible for the effect of the circular polarization of the exciting radiation on the photoemission spectra, for example, the partial loss of the elements of space symmetry due to the influence of the surface and the finite electron escape depth. This paper is devoted to the study of the influence of this type of factors that are not related to the magnetic and/or spin states of atoms. For this purpose, we have studied the intercalation compound $Fe_{1/4}TiTe_2$ in which iron atoms do not undergo magnetic ordering (at least, down to a temperature of 50 K [2]) or structural ordering that could lead to a reconstruction of the Brillouin zone of the host lattice of the $TiTe_2$ chalcogenide. However, the iron atoms reside in the spin-polarized states [1, 3]. Thus, this material is convenient for use in the investigation of possible factors that are responsible for the dichroism but not related to the spin polarization of electrons.

2. SAMPLE PREPARATION AND EXPERIMENTAL TECHNIQUE

Single crystals of the Fe_xTiTe_2 compounds were grown by the gas-transport reaction method with the use of gaseous iodine I_2 as a gas carrier. The growth technique was similar to that used for growing M_xTiSe_2 crystals in our earlier work [4]. The chemical composition of the crystals was determined using the electron microprobe analysis with a JEOL-733 microscope and, according to the lattice parameters [2], corresponded to the formula $Fe_{1/4}TiTe_2$.

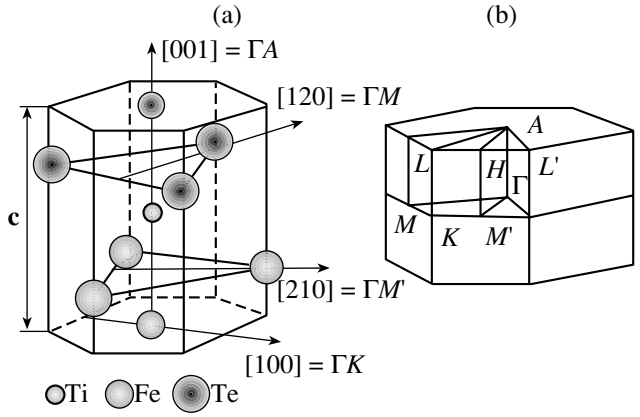

Fig. 1. (a) Fragment of the $Fe_{1/4}TiTe_2$ crystal. (b) Brillouin zone of the 1*T*-$TiTe_2$ compound. The Γ*A* direction in the Brillouin zone corresponds to the direction of the **c** axis perpendicular to the basal plane of the crystal in the direct space (the [001] direction).

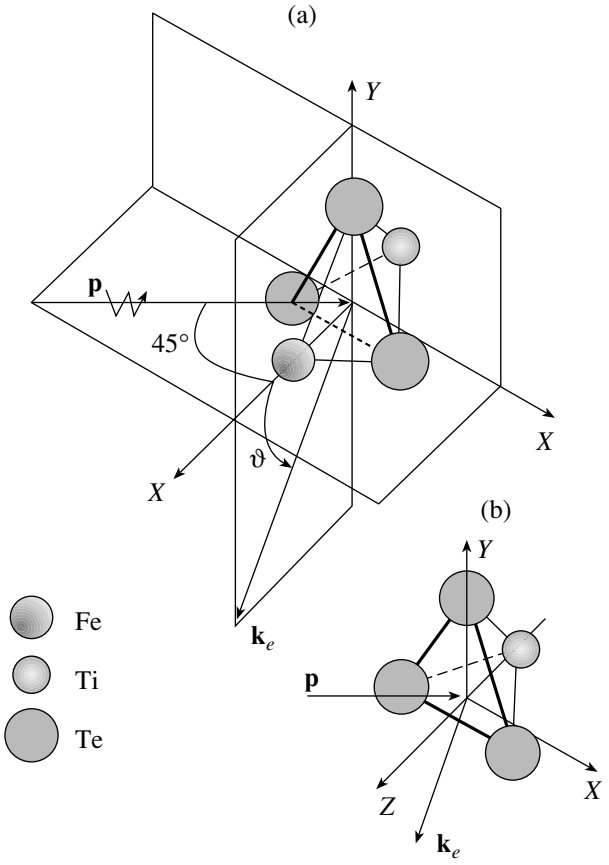

Fig. 2. Schematic diagram illustrating the performance of the experiment. Designations: **p** is the photon momentum, $\mathbf{k}_e$ is the photoelectron momentum, and ϑ is the polar angle. During the detection of photoelectrons, the polar angle changes in the *ZY* plane perpendicular to the surface of the single crystal. The *Z* coordinate axis coincides with the direction of the [001] crystallographic axis and passes through the titanium atom, the iron atom, and the center of the polyhedron. (a) Base-shared $TiTe_3Fe$ pyramids and (b) $TiTe_3$ pyramids on the surface of the single-crystal sample are shown (for more detail, see text).

The angular dependences of the photoemission (the angle-resolved photoelectron spectra) for the $Fe_{1/4}TiTe_2$ single crystal were experimentally investigated at the ELETTRA synchrotron (Trieste, Italy). The spectra were measured on a SCIENTA 50 angle-resolved spectrometer at a temperature of approximately 50 K. The excitation energy was equal to 21.5 eV. The energy resolution was 30 meV, and the cross section of the beam measured 5 × 20 μm. The experiment was performed upon excitation with circularly polarized radiation. The samples were mechanically cleaved directly in the working volume of the spectrometer (residual pressure, 10^{-9} Torr). The orientation of the samples was performed in a preparation chamber with the use of low-energy electron diffraction.

The main fragments of the crystal structure of the $Fe_{1/4}TiTe_2$ compound and the Brillouin zone are presented in Fig. 1. The schematic diagram illustrating the performance of the experiment is depicted in Fig. 2. The mutual correspondence of the most symmetric structural elements in the direct and reciprocal spaces is shown in Fig. 1. The beam of circularly polarized photons lies in the *XZ* horizontal plane and is directed at a constant angle of 45° with respect to the single-crystal surface, which coincides with the (001) crystallographic plane. During the detection of photoelectrons, the polar angle ϑ changes in the *YZ* vertical plane perpendicular to the surface of the single crystal.

According to Neumann's principle, the symmetry elements of the dichroism as a physical property of a crystal must include all the symmetry elements of the point group of the crystal and the wave vector of the valence electron. Therefore, the analysis of the behavior of the dichroism in our scheme for performing the experiment requires a detailed inclusion of the symmetry elements of the crystal, among which the glide planes play a particularly important role. In the structure of the $Fe_{1/4}TiTe_2$ chalcogenide (compound of the CdI_2 type), there exist an inversion center, two families of glide planes {001} and {100}, and one family of mirror-reflection planes {120}. These planes are perpendicular to the [110], [100], and [120] directions of the crystal, respectively (Fig. 1). These symmetry elements of the host lattice 1*T*-$TiTe_2$ are inherited by the $Fe_{1/4}TiTe_2$ intercalation compound.

3. RESULTS AND DISCUSSION

The specific feature of the angle-resolved photoelectron spectra of 2*H* and 1*T* polytypes of layered transition metal dichalcogenides, which was first noted by Smith and Traum [5], lies in a drastic difference of the intensity of electron escape in completely equivalent

(from the chemical bonding standpoint) directions Γ*M* and Γ*M*' of the Brillouin zone for the 1*T* structure as compared to the 2*H* structure. This effect was initially explained by the lowering of the symmetry of rotation around the **c** hexagonal axis to a threefold axis as compared to a sixfold axis for the 2*H* polytype and the shadow effect [5]. However, Matsushita et al. [6] calculated the photoemission dichroism for the TaS_2 compound and emphasized that the inclusion of this effect is insufficient for explaining the experimental results. According to the approximate estimates made in [5], the total escape depth is no more than 13 Å (at an excitation energy of 10.2 eV). As follows from modern data, these estimates do not correspond to reality. At an excitation energy of 20 eV, the mean free path in a similar host lattice containing transition elements does not exceed 4 Å [7]. A similar situation is observed for the 1*T*-$TiTe_2$ polytype and the $Cr_{1/3}TiTe_2$ intercalation compound [8]. This viewpoint is confirmed by the results obtained in [9, 10], according to which (angle-resolved photoelectron spectroscopic data) the ordering of intercalant 3*d* atoms in the bulk of the crystal does not result in the corresponding reconstruction of the Brillouin zone. When preparing samples for measurements, the cleavage passes through the crystallographic plane containing intercalated atoms. The surface prepared for measurements involves half of these atoms distributed in a statistically equivalent manner. In other words, the cleavage of the crystal for the preparation of a fresh surface leads to a disordered arrangement of intercalated atoms on the surface. The next undisturbed layer located at a depth of ~3.0–3.5 Å is not observed due to the absorption of photoelectrons. Under these experimental conditions, the escape of electron predominantly reflects the chemical bonding and symmetry of half the TiX_2 sandwich in the direction of the hexagonal axis (perpendicular to the surface of the single crystal). After the removal of the upper layer, the surface of the sample contains structural fragments of two types. Therefore, there occurs detection of the electrons emitted from the crystal fragments represented by $TiTe_3$ pyramids and base-shared $TiTe_3Fe$ pyramids (Fig. 2). Their quantitative ratio in the structure of the $Fe_{1/4}TiTe_2$ compound is equal to 1/8. In these polyhedra, the operations of inversion and reflection with respect to the basal plane are absent (or suppressed). In this case, the angular dependence of the photoemission from the Fe 3*d* states at a specified excitation energy is affected only by the remaining elements of space symmetry.

The titanium and tellurium atoms have the identical nearest neighbors in the second coordination sphere in the layer. Unlike these atoms, the distance between the nearest iron atoms is no less than three coordination spheres in the layer. Therefore, according to the crystal structure of the compound, the sixfold rotation axis is the main symmetry element for the titanium and tellurium atoms. For the iron atoms, the situation is qualitative different. Since the chemical bonding between intercalated iron atoms and the host lattice is weak, it is reasonable to assume that each iron atom in the iron sublattice has a rotation axis of the ∞ type with respect to the **c** axis. According to our data, the binding energy of the core levels of iron atoms remains unchanged as compared to that in metallic iron. The binding energy of the Ti $2p_{3/2}$ level for the compound under consideration is equal to 455 eV. This energy is higher than the corresponding energy in the metal by 1 eV and reflects the predominance of the ionic component in the chemical bonding of titanium in the 4+ oxidation state. Since the intensity of emission from the lower part of the $TiTe_6$ sandwich decreases sharply, the symmetry of rotation in *M* (*M*') effectively increases.

Over the entire range of polar angles, except for the angle $\vartheta = 0$, the normal **z** to the surface of the single crystal, the wave vector **p** of the incident photon, and the momentum $\mathbf{k}_e$ of the detected electron are arranged in a noncoplanar fashion. At $\vartheta = 0$, the direction of observation of photoelectrons coincides with the direction of the [001] crystallographic axis and the Γ*A* direction in the Brillouin zone (Fig. 2). As was repeatedly shown [11, 12], the dichroism observed in the noncoplanar geometry reflects the natural physical properties of an object (inherent in it), namely, the symmetry operations. If the inversion or rotation in this case is absent, the interaction of right- and left-hand polarized photons with a material is noninvariant. At $\vartheta = 0$, the geometry of the experiment is coplanar and, at this point, the matrix elements of the probability of transition of electrons to a finite state of the continuum for two types of the polarization are identical in magnitude [11]; i.e., the dichroism is absent. A change in the sign of the angle ϑ leads to a change in the sign of the dichroism, because the "dichroism" is an odd function of the electron emission angle ϑ [11].

The results of the investigation of the Fe_xTiTe_2 compound in the Γ*K* and Γ*M* directions of the Brillouin zone upon excitation by photons with opposite circular polarizations are presented in Figs. 3a and 3b. The dependences of the dichroic effect on the binding energy and the polar angle in the Γ*K* direction are plotted at the right of the Fig. 3a. The band observed immediately below the Fermi energy in both directions does not exhibit a noticeable dispersion over the entire angular range. This can mean that the spectral maximum that can be located above the Fermi energy in the unoccupied part of the valence band does not participate in the emission.

In both directions, the dichroism reaches a considerable value away from the Γ point (Figs. 3a, 3b). In the Γ*K* direction, the inversion of the intensity at different polarizations is clearly seen in the angular range in the vicinity of $\vartheta = \pm 6°$ and the binding energy range from 0 to –1 eV. At the Γ point, the dichroism is characterized by a regular behavior in accordance with the energy location of the bands (Fig. 4). The dichroism in the vicinity of the Γ point ($\Delta\varphi = 2°$) is close to zero over

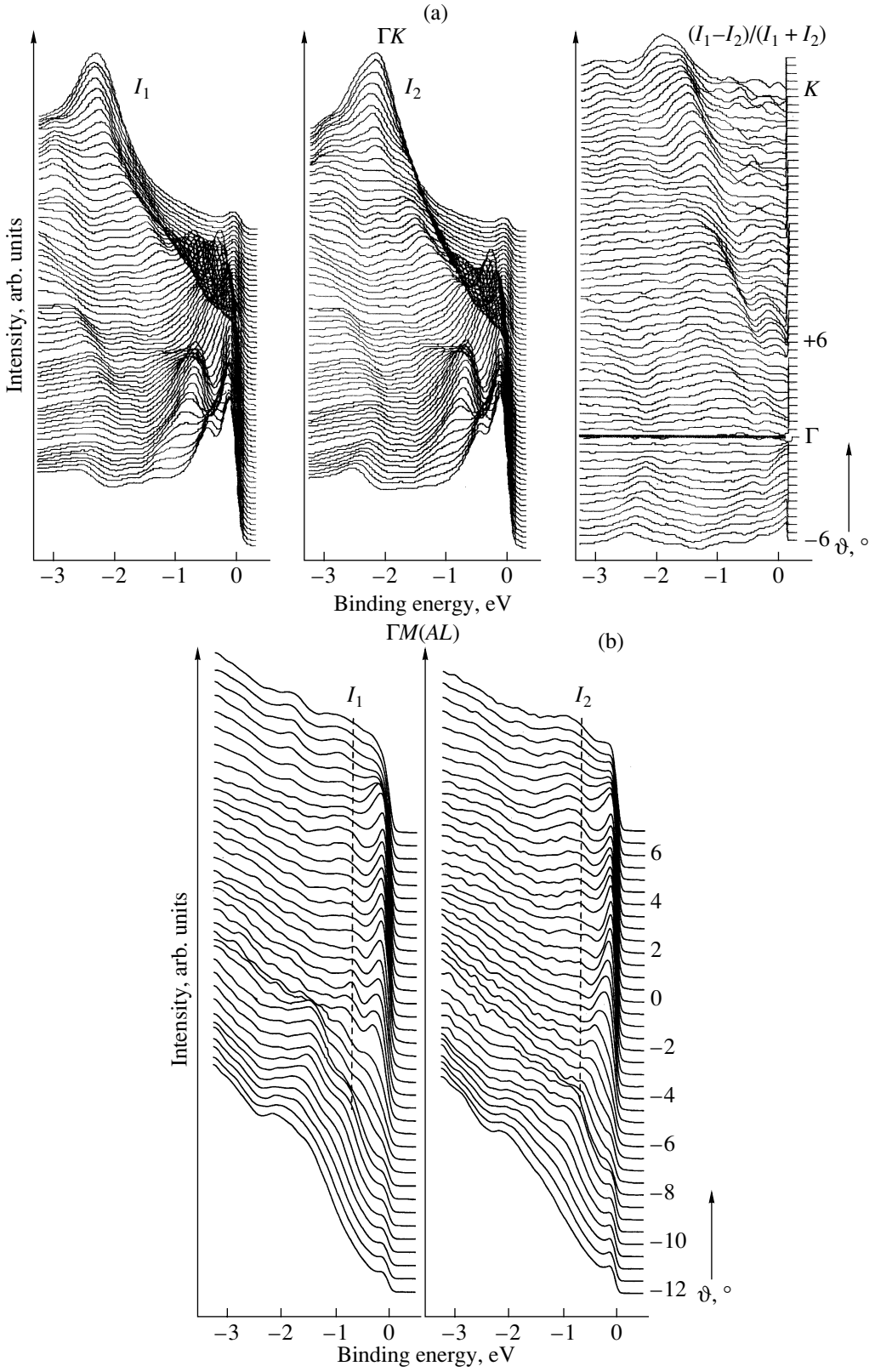

Fig. 3. (a) Angular dependences of the photoemission spectra in the Γ*K* direction upon excitation with left-hand (I_1) and right-hand (I_2) circularly polarized radiation on the binding energy. The angular distribution of the dichroism is shown at the right. At the Γ point, the polar angle is $\vartheta = 0$. (b) Angular dependences of the photoemission spectra in the Γ*M* (*AL*) direction. Dashed lines indicate the band at a binding energy of 0.7 eV with a weakly pronounced dispersion.

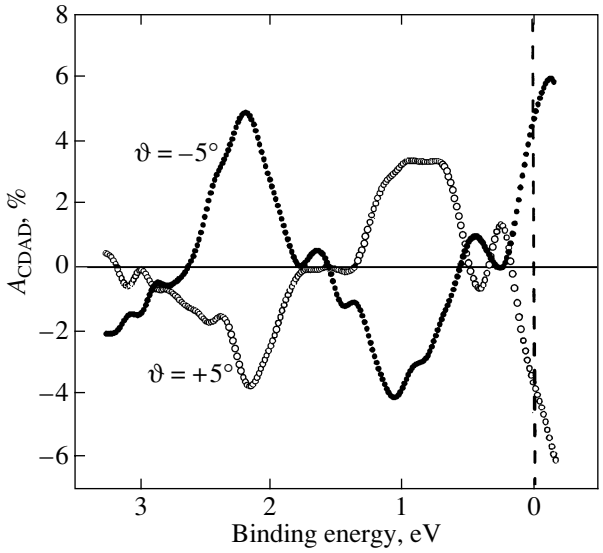

Fig. 4. Dependences of the dichroism magnitude on the binding energy in the vicinity of the Γ point in the range of the polar angle $\Delta\vartheta = \pm 5°$.

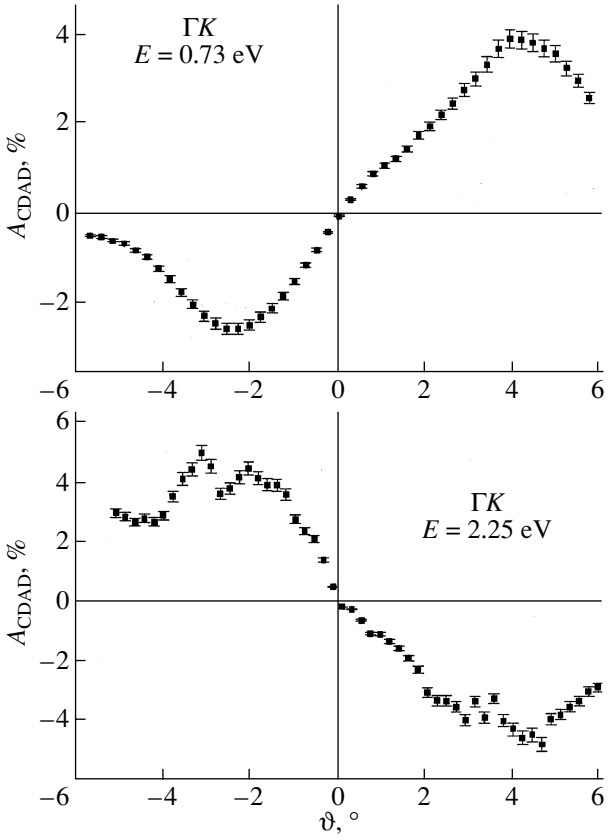

Fig. 5. Dependences of the dichroism magnitude in the Γ*K* direction for two bands with binding energies of 0.73 and 2.25 eV.

the entire range of energies (Fig. 3a). Away from the Γ point toward both positive and negative angles, the behavior of the circular dichroism in the photoemission angular distribution (CDAD) changes (Fig. 5) and this quantity can be as large as 5%. It should be noted that the circular dichroism in the photoemission angular distribution is identical in magnitude for all bands but has different signs on both sides of the Γ point. By contrast, in the vicinity of the Γ point (in the Γ*M* direction), the dichroism is an even function and reaches 15–20% in the range below the Fermi energy. In the other energy range, the circular dichroism in the photoemission angular distribution almost does not differ in magnitude from the aforementioned behavior for the Γ*K* direction. It should be noted that the experimental scheme is chosen so that the directions of the circularly polarized radiation in the projections onto the *X* and *Z* axes are opposite. This experimental feature can be used for analyzing the orbital symmetry of the experimentally determined bands and their comparison with the results of theoretical calculations. The maximum value of A_{CDAD} in the Γ*K* direction is equal to 15%. The effects associated with the energy resolution lead to a seeming shift in the dichroism with respect to the location corresponding to the maximum intensity of the bands observed in the spectra.

The mechanism of manifestation of the circular dichroism and its angular dependence in the photoemission has been considered in a number of theoretical works (see, for example, [11–13]). As follows from the corresponding calculations, the circular dichroism in the photoemission angular distribution reflects the interaction of circularly polarized photons with the total angular momentum of the excited atom and is observed irrespective of the magnetic state of samples. According to model calculations, one of the factors responsible for the circular dichroism in the photoemission angular distribution is the interference of the corresponding final states with the projections of the angular momenta $l + 1$ and $l - 1$. This interpretation is in agreement with the results obtained from the theoretical calculations of the angular dependence of the photoemission in [6] for the TaS_2 compound upon excitation with the circularly polarized radiation. It should be noted that, in the calculations performed in [6], the model conditions for recording were far from real.

One more feature of the spectra of the Fe_xTiTe_2 compound is the appearance of an additional almost dispersionless band with a binding energy of 0.78 eV in the Γ*M* direction (Fig. 3b). According to the band calculations [1], this band is associated with the Fe 3*d*–Ti 3*d* hybridization and is spin-polarized. In pure unintercalated compound, this band was not revealed [8].

The effect of the appearance and suppression of the dichroism is especially pronounced upon change in the angular range in the vicinity of the Γ point in the Γ*K* direction (Figs. 3–5). At the Γ point, there are bands with binding energies of 0.1, 0.7, 1.7, and 2.2 eV (Fig. 3a). As was noted above, the upper band incompletely manifests itself in the spectrum of occupied

Binding energies E (eV) of the Fe3d bands for the $FeTi_4Te_8$ compound according to the results of theoretical calculations in the vicinity of the Γ point and the experimental data

No.	Fe3d ↑			Fe3d ↓			Experiment
	d_{xz+yz}	$d_{x^2y^2+xy}$	d_{z^2}	d_{xz+yz}	$d_{x^2y^2+xy}$	d_{z^2}	
1				0–0.3			0–0.3
2					0.6		0.7–1.0
3	1.0	1.0–1.2				1.2	1.25
4			2.3				2.3
	(*YZ*), (*XY*), (*XZ*)	(*XZ*), (*YZ*), (*XY*)	(*XY*)				

Note: The symmetry planes for orbitals in the global coordinate system shown in Fig. 2 are given in the lower row. All symmetry planes are glide planes, except for the *YZ* plane in the case where the [120] (Γ*M*) direction coincides with the *Z* axis. Arrows indicate spin-up and spin-down directions. The symmetry of the experimentally observed bands in the spectra was identified taking into account their energy position and power (filling) obtained in calculations, superposition of bands associated with the orbitals of different symmetries, and the behavior of the dichroism in the vicinity of the Γ point.

states and, hence, inadequately reflects the dichroic effect. The positions of the other three bands are clearly determined (Fig. 3a). The qualitative difference in the behavior of the dichroism in the ΓK and ΓM directions due to the difference in their symmetry in the Brillouin zone is of special interest. In dichalcogenides, the intercalated atoms, for the most part, determine the physical properties. In this respect, we are interested in the Fe 3d states and their distribution in the **k** space.

The electronic structure was calculated in the framework of the density functional theory with the use of the full-potential augmented-plane-wave method implemented in the WIEN2k code [14]. The titanium dichalcogenide doped with iron atoms (one atom per four formula units) was simulated by a periodic supercell with a hexagonal structure (space group P–3m1, no. 164) with the experimentally determined lattice parameters $a = 2 \times 3.8109$ Å and $c = 6.345$ Å and the atomic coordinates Fe(0, 0, 1/2), Ti(0, 0, 0), 3 × Ti(1/2, 0, 0), 6 × Te(1/6, 5/6, z), and 2 × Te(2/3, 1/3, z) with the inner parameter $z = 0.2652$. The exchange–correlation potential was chosen within the local-spin density approximation. The periodicity of the used supercell formally corresponds to the ferromagnetic ordering of magnetic moments of iron atoms. However, owing to the large distance between the iron atoms, their interaction is very weak and localized states characteristic of magnetic impurities manifest themselves in the electronic structure of iron atoms.

The dispersion curves E(**k**) for the Fe 3d states with different orbital symmetries according to the model calculations of the electronic structure for the $Fe_{1/4}TiTe_2$ compound are depicted in Fig. 6. It should be noted that, as follows from the data obtained in our previous work [15], in which the valence bands of Fe_xTiTe_2 single crystals with different iron contents were investigated by x-ray photoelectron spectroscopy, the Fe 3d states are located in the energy range from –2.5 to 0 eV below the Fermi level. Therefore, we restrict our analysis of the spectra to this energy range. The calculated electronic structure E(**k**), including the Fe 3d states, is presented in Fig. 6. The theoretical and experimental binding energies for the bands corresponding to different orbital symmetries are listed in the table. The mirror-reflection planes for these bands in the chosen coordinate system (Fig. 2) are given in the lower row of the table. The experimentally observed dependence of the dichroism on the binding energy in the valence band is plotted in Fig. 3. As was noted above, the inversion of the dichroism sign away from the Γ point is associated with the odd behavior of the dichroism.

The energy positions of the Fe 3d orbitals in the vicinity of the Γ point are presented in the table. The orbitals located in the upper part of the occupied band, in order of increasing binding energy, are $3d_{xz+yz}$, $3d_{x^2y^2+xy}$, and the lower orbital $3d_z^2$. It can be seen from the table and the curves E(**k**) shown in Fig. 6 that the orbitals $3d_{x^2y^2+xy}$ and $3d_{xz+yz}$ with spin-up are mixed at the Γ point. The spin-down orbital $3d_{x^2y^2+xy}$ and the spin-up orbital $3d_z^2$, which according to the calculations are not mixed with other Fe 3d orbitals at the Γ point, are most close in energy to the experimentally observed bands with the energies $E = 0.73$ and 2.25 eV (Fig. 4), respectively. The dichroism signs for these bands are opposite to each other. Although the spin-down orbital $3d_{x^2y^2+xy}$ and the spin-up orbital $3d_z^2$ have different spin polarizations, this in the given case is not related to the behavior of the dichroism because of the reasons discussed above. In our opinion, the difference in the dichroism of these bands is associated with the difference in the space symmetry of the corre-

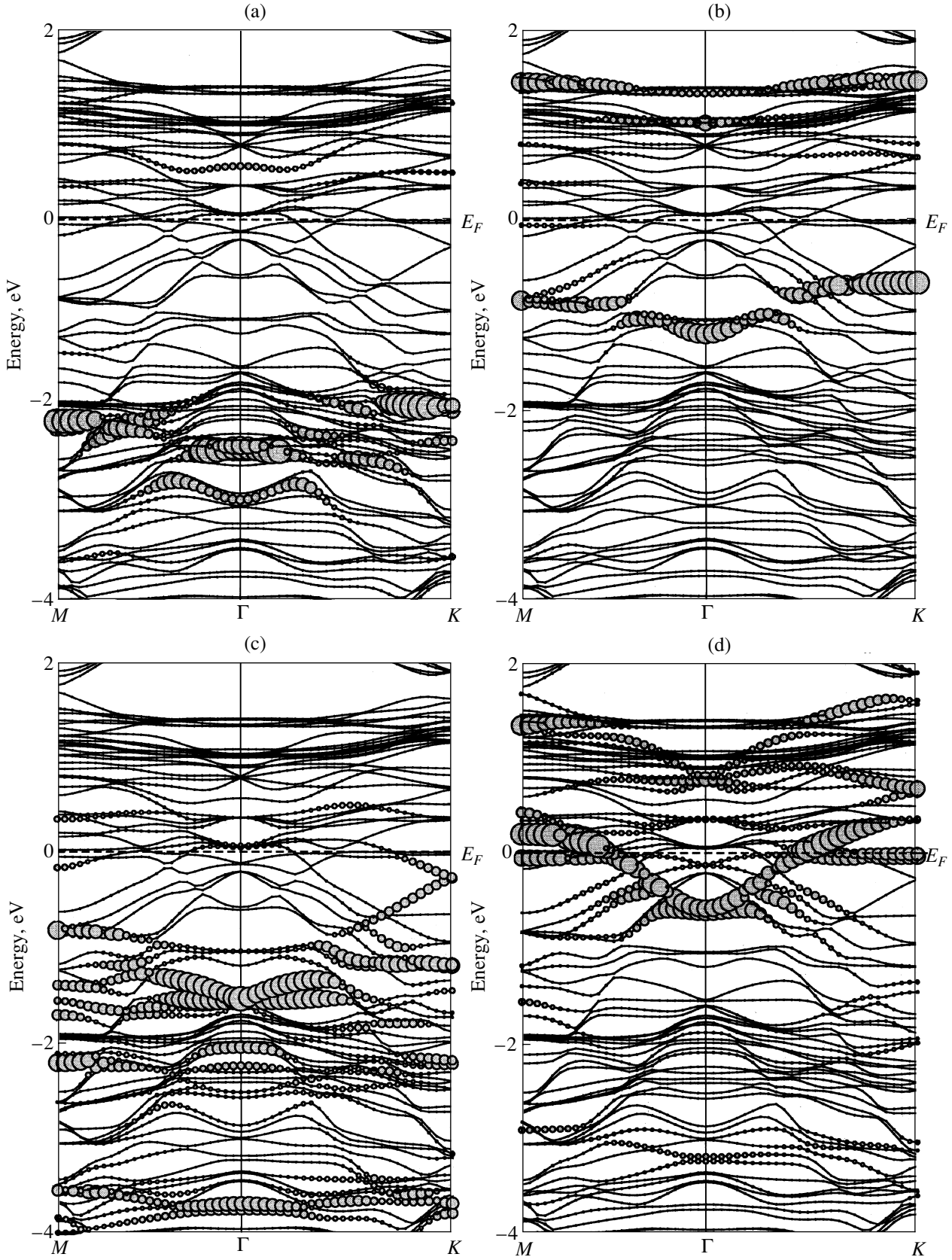

Fig. 6. Results of the calculation for the Fe 3*d* states in the $Fe_{1/4}TiTe_2$ crystal: (a) d_z^2 with spin-up, (b) d_z^2 with spin-down, (c) $d_{x^2y^2+xy}$ with spin-up, and (d) $d_{x^2y^2+xy}$ with spin-down.

sponding orbitals with respect to the coordinate system related to the crystal (Fig. 2). In this coordinate system, the principal rotation axes of the orbitals under consideration are parallel to the *Z* axis. The projections of the photon momentum onto the *XY* and *YZ* coordinate planes have opposite signs; i.e., the circular polarizations along the positive directions of the *X* and *Z* axes are opposite to each other. Therefore, if the mutually perpendicular planes *XZ* and *XY* for the spin-down orbital $3d_{x^2y^2+xy}$ and the spin-up orbital $3d_z^2$ are the reflection planes, the electrons of the corresponding orbitals are excited by radiation with the opposite circular polarizations and the dichroism signs for them are opposite to each other. The electron density cross section parallel to the **c** axis for $Me_x TiSe_2$ crystals (*Me* = Cr, Co) was theoretically calculated in [1]. It follows from this cross section that the 3*d* electrons of the *Me* atoms are strongly polarized toward the Se atoms and the chemical bonding between the intercalated and Se atoms is provided through the hybridized $Me3d_{(x^2-y^2),\,xy,\,xz,\,yz}$ orbitals. Since the Fe atoms under the experimental measurement conditions are located at the crystal surface, the branches of these orbitals are asymmetric with respect to the *XY* plane. Therefore, the *ZY* plane is the reflection plane for these atoms. The Fe $Fe3d_z^2$ orbital almost does not participate in the chemical bonding, and its symmetry is similar to atomic. As a consequence, the *XY* plane is the main reflection plane.

The results of our investigations make it possible to perform the corresponding analysis and to predict, to some extent, the behavior of the intensity of the spin-polarized bands of the Fe_xTiTe_2 crystal with the ordered magnetic sublattice of iron in an external magnetic field. In this case, too, there should arise a dichroism caused by the chirality of the object and its magnitude should depend on the direction of the magnetic induction vector in the sample. When ordering the magnetic moments in the sublattice of intercalated atoms, there can arise additional reflection planes. This will lead to a change in the dichroism sign for the corresponding subbands.

4. CONCLUSIONS

Thus, the dichroism of the emission of valence electrons from the $Fe_{1/4}TiTe_2$ crystal was experimentally measured upon excitation by circularly polarized synchrotron radiation with an energy of 20.5 eV. This radiation simulates a typical source of ultraviolet radiation of He atoms. Upon excitation with the aforementioned energy, the angular dependence of the spectra partially loses information on the symmetry of the crystal, including the orbitals of valence electrons. The reason is that the mean free path of photoelectrons in the crystal is relatively small and does not exceed the size of the unit cell, which has all symmetry elements. This is especially true for low-symmetry systems, such as quasi-two-dimensional dichalcogenides. This seeming incompleteness of the spectral data allows one to determine the orbital symmetry of some bands. We revealed the angular dependence of the dichroism of individual bands, which, according to the data obtained from theoretical calculations, are predominantly formed by the Fe 3*d* states. It was established that the angular dependence of these bands is determined by the space symmetry of the crystal and the molecular orbitals of the Fe 3*d* electrons.

ACKNOWLEDGMENTS

We would like to thank V.I. Grebennikov for his participation in discussions of the results.

This study was performed within the framework of the Project No. 2004105 at the ELETTRA synchrotron (Trieste) and supported by the Ministry of Education and Science of the Russian Federation with the program "Development of the Scientific Potential of the Higher School" (project no. RNP.2.1.1.6945) and the Russian Foundation for Basic Research (project no. 06-03-32900).

REFERENCES

1. A. V. Postnikov, M. Neumann, St. Plogmann, Yu. M. Yarmoshenko, A. N. Titov, and A. V. Kuranov, Comput. Mater. Sci. **17**, 450 (2000).
2. V. G. Pleshchev, A. N. Titov, S. G. Titova, and A. V. Kuranov, Neorg. Mater. **33** (11), 1333 (1997) [Inorg. Mater. **33** (11), 1128 (1997)].
3. X. Y. Cui, H. Negishi, S. G. Titova, K. Shimada, A. Ohnishi, M. Higashiguchi, Y. Miura, S. Hino, A. M. Jahir, A. Titov, H. Bidadi, S. Negishi, H. Namatame, M. Taniguchi, and M. Sasaki, Phys. Rev. B: Condens. Matter **73**, 085111 (2006).
4. A. N. Titov, A. V. Kuranov, V. G. Pleschev, Yu. M. Yarmoshenko, M. V. Yablonskikh, A. V. Postnikov, S. Plogmann, M. Neumann, A. V. Ezhov, and E. Z. Kurmaev, Phys. Rev. B: Condens. Matter **63**, 035106 (2001).
5. N. V. Smith and M. M. Traum, Phys. Rev. B: Solid State **11**, 2087 (1975).
6. T. Matsushita, S. Imada, H. Diamon, T. Okuda, K. Yamaguchi, H. Miyagi, and S. Suga, Phys. Rev. B: Condens. Matter **56**, 7687 (1997).
7. C. J. Powell and A. Jablonski, J. Phys. Chem. Ref. Data **28**, 19 (1999).
8. T. V. Kuznetsova, M. V. Yablonskikh, A. V. Postnikov, G. Nicolay, B. Eltner, F. Reinert, Y. M. Yarmoshenko, A. N. Titov, and J. Nordgren, J. Electron Spectrosc. Relat. Phenom. **137–140**, 481 (2004); T. V. Kuznetsova, A. N. Titov, Yu. M. Yarmoshenko, E. Z. Kurmaev, A. V. Postnikov, G. Pleschev, B. Eltner, G. Nicolay, D. Ehm, S. Schmidt, F. Reinert, and S. Hüfner, Phys. Rev. B: Condens. Matter 72, 085418 (2005).

9. T. Matsushita, S. Suga, Y. Tanake, H. Shigeoka, T. Nakatani, T. Okuda, T. Terauchi, T. Shishidou, A. Kimura, H. Daimon, S.-J. Oh, A. Kakizaki, Toyohiko Kinoshita, H. Negishi, and M. Inoue, J. Electron Spectrosc. Relat. Phenom. **78**, 477 (1996).
10. H. Martinez, Y. Tison, I. Baraile, M. Loudet, and D. Gonbeau, J. Electron Spectrosc. Relat. Phenom. **125**, 181 (2002).
11. R. L. Dubs, S. N. Dixit, and V. McKoy, Phys. Rev. Lett. **54**, 1249 (1985).
12. D. Venus, Phys. Rev. B: Condens. Matter **56**, 2661 (1997).
13. D. Venus, W. Kuch, A. Dittschar, M. Zharnikov, C. M. Schneider, and J. Kirschner, Phys. Rev. B: Condens. Matter **52**, 6174 (1995).
14. P. Blaha, K. Schwarz, P. Sorantin, and S. B. Trickey, Comput. Phys. Commun. **59**, 339 (1990); http://url.wien2k.at.
15. A. N. Titov, S. G. Titova, M. Neumann, V. G. Pleschev, Yu. M. Yarmoshenko, L. Krasavin, A. Dolgoshein, and A. Kuranov, Mol. Cryst. Liq. Cryst. **311**, 161 (1998).

Translated by O. Borovik-Romanova

SPELL: OK